RESTORATION ECOLOGY
The Journal of the Society for Ecological Restoration

RESEARCH ARTICLE

Demography with drones: detecting growth and survival of shrubs with unoccupied aerial systems

Peter J. Olsoy[1,2], Andrii Zaiats[3], Donna M. Delparte[4], Matthew J. Germino[5], Bryce A. Richardson[6], Anna V. Roser[3], Jennifer S. Forbey[3], Megan E. Cattau[7], T. Trevor Caughlin[3]

Large-scale disturbances, such as megafires, motivate restoration at equally large extents. Measuring the survival and growth of individual plants plays a key role in current efforts to monitor restoration success. However, the scale of modern restoration (e.g., >10,000 ha) challenges measurements of demographic rates with field data. In this study, we demonstrate how unoccupied aerial system (UAS) flights can provide an efficient solution to the tradeoff of precision and spatial extent in detecting demographic rates from the air. We flew two, sequential UAS flights at two sagebrush (Artemisia tridentata) common gardens to measure the survival and growth of individual plants. The accuracy of Bayesian-optimized segmentation of individual shrub canopies was high (73–95%, depending on the year and site), and remotely sensed survival estimates were within 10% of ground-truthed survival censuses. Stand age structure affected remotely sensed estimates of growth; growth was overestimated relative to field-based estimates by 57% in the first garden with older stands, but agreement was high in the second garden with younger stands. Further, younger stands (similar to those just after disturbance) with shorter, smaller plants were sometimes confused with other shrub species and bunchgrasses, demonstrating a need for integrating spectral classification approaches that are increasingly available on affordable UAS platforms. The older stand had several merged canopies, which led to an underestimation of abundance but did not bias remotely sensed survival estimates. Advances in segmentation and UAS structure from motion photogrammetry will enable demographic rate measurements at management-relevant extents.

Key words: drones, plant demography, sagebrush, segmentation, stand age structure, structure from motion photogrammetry

Implications for Practice

- Monitoring is vital for successful restoration. Remote sensing is needed to monitor restoration outcomes across broad scales, and unoccupied aerial systems (UAS) provide a valuable tool for individual plant-level measurements relevant to long-term restoration success.
- Stand age structure impacted our ability to accurately estimate demography, including crown-to-crown matching. Stand age and integration of multispectral sensors should be considered when implementing this workflow for restoration applications.
- Monitoring restoration with UAS is feasible for performing a complete census, but not yet for growth. There is a startup cost for equipment ($1000–$25,000) and training that needs to be overcome before time-savings and efficiency can make UAS cost-effective as a monitoring tool.

Introduction

As anthropogenic change leads to habitat loss and degradation over increasingly larger areas, predicting ecosystem recovery after disturbance is crucial. Spatial variation in plant demographic rates is a fundamental reason some ecosystems recover while others remain degraded (Albrecht & McCue 2010; Caughlin et al. 2016; Shriver et al. 2019). Bottlenecks that prevent plant population recovery can occur across multiple demographic rates, including growth, survival, and reproduction (Holl 1999). Demographic bottlenecks are particularly important for small populations, where demographic stochasticity can exacerbate impacts of the environment on population growth rates (Godefroid et al. 2011). Identifying and mitigating these demographic bottlenecks by monitoring plant performance can allow for spatially explicit predictions of recovery potential and aid

Author contributions: PO, AZ, DD, MG, BR, JF, MC, TC conceived the ideas and designed methodology; DD, AZ, MG, AR collected the data; PO, AZ, AR, TC analyzed the data; PO, AZ, TC led the writing of the manuscript; all authors contributed critically to the drafts and gave final approval for publication.

[1]USDA Agricultural Research Service, 67826-A Hwy 205, Burns, OR 97720, U.S.A.
[2]Address correspondence to P. J. Olsoy, email peter.olsoy@usda.gov
[3]Department of Biological Sciences, Boise State University, 1910 W University Dr, Boise, ID 83725, U.S.A.
[4]Department of Geosciences, Idaho State University, 921 S 8th Ave, Pocatello, ID 83209, U.S.A.
[5]U.S. Geological Survey, Forest and Rangeland Ecosystem Science Center, 230 N Collins Rd, Boise 83702, ID, U.S.A.
[6]USDA Forest Service, Forest Sciences Laboratory, 1221 S Main St, Moscow, ID 83843, U.S.A.
[7]Human-Environment Systems, Boise State University, 1910 W University Dr, Boise, ID 83725, U.S.A.

doi: 10.1111/rec.14106

adaptive management, including resource allocation to maximize project success and avoid repeating ineffective restoration techniques (James et al. 2011; Caughlin et al. 2019). The most informative scale to measure demographic rates is at the scale of individual plants, as individual-level differences, including size, genotype, and physiological and health status, underlie long-term population trajectories (Merow et al. 2014). However, measuring individual plant demography presents a challenge at spatial extents that match areas impacted by large disturbances. Insufficient monitoring of large-scale restoration projects is a consequence of this challenge, resulting in uncertain and unknown outcomes for many planting initiatives (Holl & Brancalion 2020).

Remote sensing could provide a solution to the scale mismatch between landscape-level disturbance and individual plant measurements. High-resolution remotely sensed data can now detect individual plants over areas that far exceed the scale of field plots (e.g., >1 ha). For medium to large-sized trees, satellite imagery provides sufficient resolution to detect individuals at continental scales (Brandt et al. 2020). For smaller plants, such as shrubs or bunchgrasses, the increasing availability of unoccupied aerial systems (UAS) is enabling maps of species abundance at landscape scales (Rominger & Meyer 2019; Gillan et al. 2020). UAS structure from motion photogrammetry provides a low-cost solution to capture canopy structure of individual plants, previously only available with high-cost LiDAR data collections, unlocking the potential to accurately measure plants across the landscape (Anderson & Gaston 2013). The capacity to detect plant species at management-relevant extents has the potential to transform restoration efforts, from mapping early-successional species indicative of restoration success (Williams et al. 2022) to measuring the abundance of rare species in heterogeneous landscapes (Rominger & Meyer 2019). Beyond mapping plants at a single time step, advances in remote sensing raise the question of whether plant demographic rates could be estimated from time series of remotely sensed data.

Several studies have demonstrated the feasibility of estimating plant growth and survival using remote sensing. The most straightforward approach to estimating plant demography is to overlay hand-digitized outlines of plant crowns across time periods (Stears et al. 2022). However, manual digitization is not feasible across large scales that encompass >100,000 of individual plants. An alternate solution is the application of structural measurements, such as aerial LiDAR, that enable automated segmentation of individual crowns (Tompalski et al. 2021). For example, Beese et al. (2022) applied repeat airborne LiDAR to map oil palm growth, enabling growth estimates for >500,000 individual plants that encompassed landscape-level environmental gradients. Despite the promise of repeat airborne data for quantifying demographic rates, several obstacles remain in linking remote sensing measurements of crowns across time periods.

Unlike field measurements, where individual plants can be tagged and re-measured, remote measurements of growth and survival rely on matching crowns from the same individual across different time steps. Crown-to-crown matching often results in error, due to spatial uncertainty in remote sensing data compounded by demographic changes that alter the spatial position and structure of crowns across time periods (Zhao et al. 2018; Marconi et al. 2022). For example, individual trees scattered over predominantly treeless landscapes may be easier to detect and match, compared to densely populated forested areas. Segmentation algorithms, which automatically delineate individual crowns, are the first step in crown-to-crown matching. Overlapping crowns and disjunct branches of the same plant provide examples where segmentation could result in either under or over-segmentation. Optimizing segmentation involves tradeoffs between accurate counts of plant crowns and accurate measurements of individual crown size (Williams et al. 2020; Qin et al. 2022). Furthermore, matching crowns through time raises the issue of error propagation, as inaccuracies at single time steps compound over multiple time steps (Peter & Messina 2019), particularly if the wrong pair of crowns are continually misidentified as the same plant. Exploring these tradeoffs, including quantifying error in linking remote sensing products across time periods, will be essential to operationalize remote measurements of growth and survival for restoration applications.

Along with the inherent challenges of crown-to-crown matching, changing environmental context poses a particular challenge for remote measurements of plant demography during ecosystem recovery. Changing biotic factors, such as plant succession, affect remote sensing via structural and spectral differences over time (Kalacska et al. 2007). These changes can confuse the classification of plants with similar structures (Osinska-Skotak et al. 2019). For example, herbivory can reduce vegetative biomass relative to plant growth (Sankey et al. 2016), potentially resulting in errors when monitoring demography with remote sensing. The utility of remote sensing for monitoring plant populations during ecosystem restoration will depend on whether crown-to-crown matching algorithms are robust across different successional stages. Nevertheless, few studies have explored how differences in stand development influence the accuracy of remote sensing algorithms.

Efforts to measure demography with remote sensing, including improving crown-to-crown matching algorithms and developing transferable techniques for change detection across successional environments, have largely focused on trees. For other functional groups, including shrubs in dryland ecosystems that represent 40% of the earth's landmass (Hoover et al. 2020), and have critical importance for restoration efforts, aerial demography remains underdeveloped. We aim to explore the feasibility of UAS-derived estimates of growth and survival for sagebrush (Artemisia tridentata), a semi-arid shrub that is central to ecosystem restoration efforts in the North American West. Sagebrush is a foundational species in the vast sagebrush-steppe ecosystem, which once covered 8% of the continental U.S. but is increasingly threatened by changing fire regimes, invasive species, and land development (Requena-Mullor et al. 2023). These disturbances have prompted equally vast restoration efforts, including the purchase of >$100 million in sagebrush seed for restoration efforts by the U.S. government during the last century (Pilliod et al. 2017; Simler-Williamson & Germino 2022). High variability in restoration outcomes is the

norm across sagebrush steppe, motivating the need for scalable monitoring techniques (Germino et al. 2022). While medium-resolution satellite products are increasingly used to forecast trajectories of sagebrush cover after disturbance (Simler-Williamson & Germino 2022; Zaiats et al. 2023), the 30-m resolution of these products cannot represent individ-ual sagebrush plants. For sagebrush, individual-level measurements are key, given high levels of between-plant genetic variation with relevance for local adaptation (Richardson & Chaney 2018; Davidson & Germino 2020), differences in recovery trajectories depending on individual plant sizes (Shriver et al. 2019), and reliance on individual species, patch, and plant traits by vertebrate herbivore species of conservation concern (Frye et al. 2013; Ulappa et al. 2014; Fremgen-Tarantino et al. 2020).

In this study, we applied structural measurements from UAS platforms to detect individual sagebrush plants and measure their growth and survival. Our study took place in sagebrush common gardens, where individual plants represent genetic diversity from source populations across sagebrush ecosystems, and where complete field censuses provide an ideal ground-truthed comparison with remotely sensed data. The sagebrush common gardens parallel active restoration projects that rely upon planting seedlings, resulting in relatively simple and homogenous stand structure, compared to naturally regenerating landscapes. We first determined the accuracy of crown detection algorithms, including tradeoffs between the accuracy of total counts and crown area. We then used data from repeat flights to develop crown-to-crown matching algorithms, which we applied to measure growth and survival between two censuses. Finally, we asked how the accuracy of our algorithms changed across stand development by replicating our efforts across common gardens that varied in planting date, including a garden in the early stages of stand development with small outplants and a garden in the later stages of stand development where outplants experienced a decade of growth and mortality. Altogether, our study represents a step toward building the capacity to monitor plant demography with remotely sensed data.

Methods

Overview

We investigated how UAS technologies and structure from motion photogrammetry can be used to monitor the growth and survival of individual sagebrush plants at two experimental field sites in Southwest Idaho, USA (Fig. 1). After we acquired temporal UAS data at two time steps from each site, we processed the raw imagery using structure from motion algorithms and generated canopy height models (CHMs) for each site and census date. Each CHM was independently used to detect individual plants using canopy detection algorithms

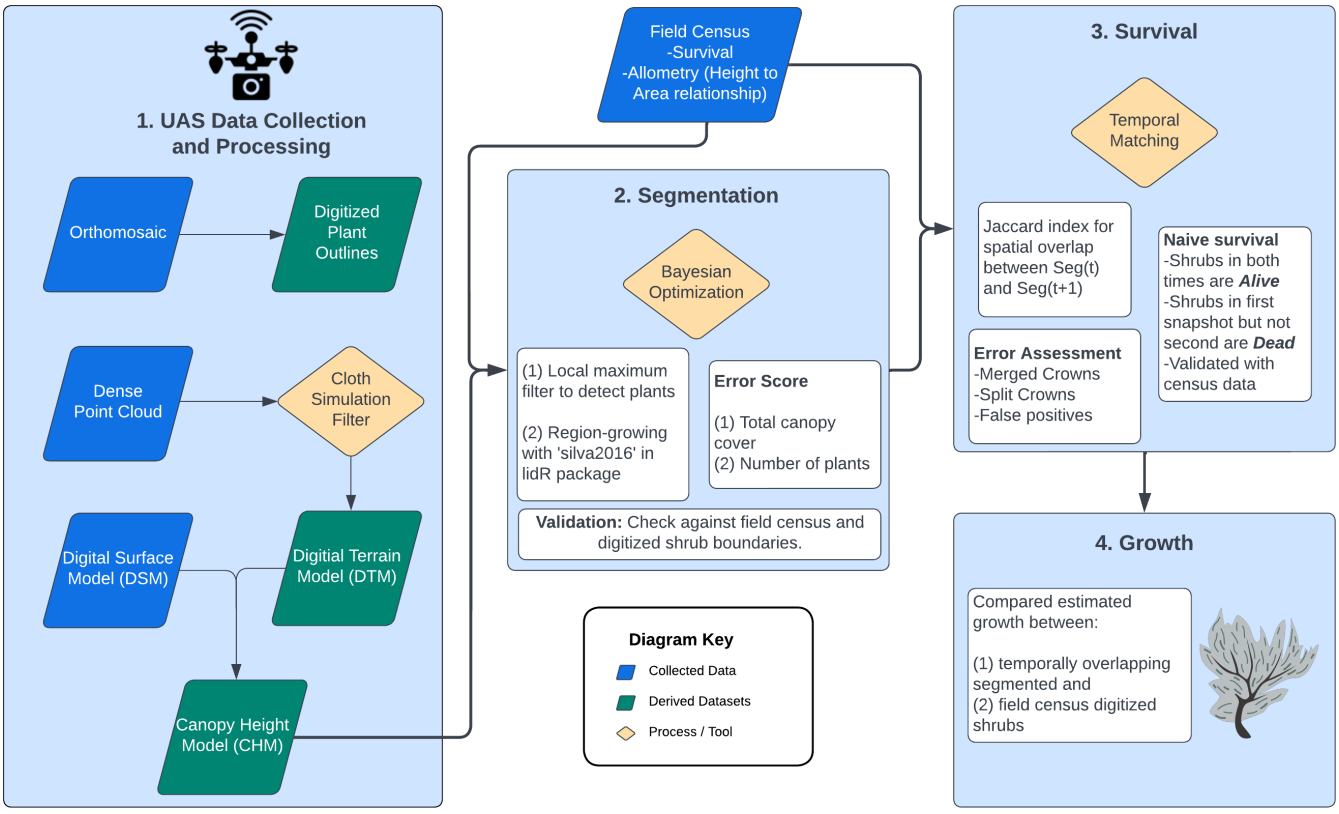

Figure 1. Workflow diagram showing the data collection, image processing, and structure from motion photogrammetry, segmentation, survival, and growth estimations with unoccupied aerial system (UAS) structural data.

(Young et al. 2022). We then used a crown-to-crown matching algorithm to identify the same plant across multiple time steps. We measured growth by comparing crown size from year to year for surviving individual plants. To validate our products, we compared the automatically detected plants to field-validated plant locations and hand-digitized plant crowns from each census.

Study Sites and Field Data Collection

Our study areas represent two big sagebrush (A. tridentata) field experiments, that is, common gardens, located in the Great Basin cold-desert ecosystem with plants representing three subspecies (A. t. tridentata, A. t. vaseyana, A. t. wyomingensis). Each common garden is a field plot with A. tridentata plants organized in a grid with regular spacing along the x and y dimensions. Besides the focal A. tridentata plants, the common gardens included small shrub recruits, perennial and annual grasses and forbs, and bare ground. The first common garden is the Orchard common garden (43.322 N, 115.998 W, 26 m 26 m, hereafter Orchard garden) established in 2010 and originally contained 468 plants, with the rows separated by 1 and 1.5 m along x and y, respectively (Fig. 2). During the first field census in 2015, there were 313 plants, with a subse-quent mortality decline to 219 plants by the time of the second field census in 2019. The Soda common garden (43.300 N, 116.991 W, 38 m 42 m, hereafter Soda garden) was a larger experiment established in 2015 (Davidson & Germino 2020). The Soda garden included 1365 plants with minimal subsequent mortality during 2019 and 2021 field censuses, containing 1217 and 1209 live plants, respectively. Plants were separated by 1.5 m. Field measurements entailed standardized surveys of each plant in the common gardens, where a plant was recorded as either dead or alive, and size measured as the maximum crown height (not including flowering stalks), longest width, and crown width perpendicular to the longest axis.

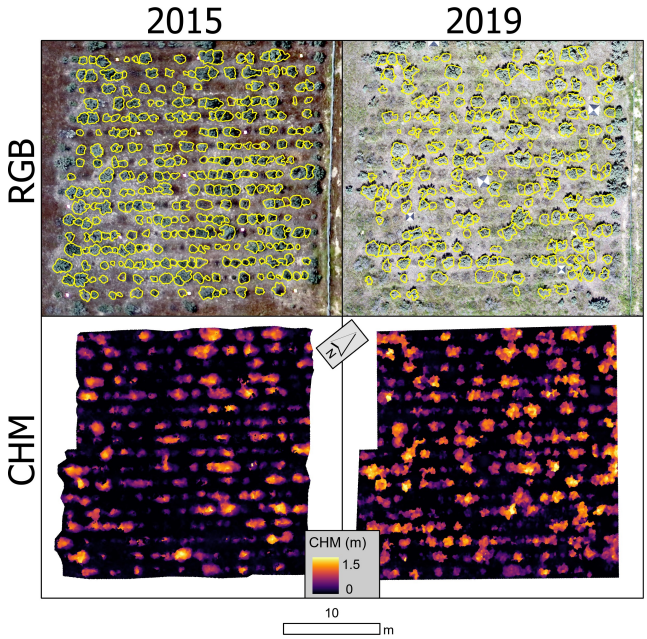

Figure 2. UAS true color (RGB) orthomosaic and CHM for the Orchard common garden in Idaho, USA during two census time steps in 2015 and 2019. This common garden represented a more established (2010) big sagebrush (Artemisia tridentata) population with larger individuals and had experienced a large dieoff of >100 plants between censuses.

UAS Data Collection and Processing

We collected UAS data on two dates at each garden using a rotor copter UAS equipped with a true color (i.e., Red-Green-Blue [RGB]) camera and pre-programmed flight missions (Table 1). Flights coincided with field censuses in 2015 and 2019 for the Orchard garden, and 2019 and 2021 for the Soda garden. To improve the geopositioning accuracy of the final products and the quality of the structure from motion reconstruction, each flight included a set of ground control points (GCPs) that were mapped with a survey-grade global positioning system (GPS) unit (HiPer-V, Topcon Positioning System, Inc). The points were registered for 30 seconds and later post-processed using Online Positioning User Service (OPUS, https://geodesy.noaa.gov/OPUS/) and Topcon Magnet Tools. We established 5–10 GCP for each UAS flight using a series of targets, including small circular targets, tarp targets, and scale bars.

Each flight mission produced a set of RGB images we processed using the structure from motion algorithm and georeferenced using ground control points following the protocol from Roser et al. (2022). The output products included a dense point cloud and a Digital Surface Model (DSM) for each common garden. To create a CHM, we generated a digital terrain model (DTM = DSM vegetation) and then subtracted DTM from DSM to obtain the CHM. To generate a DTM from the dense cloud, we applied a Cloth Simulation Filter (CSF) algorithm with subsequent point filtering curvature statistics to classify each point as ground or vegetation (CloudCompare version 2.13; https://github.com/andriizayac/uas_data_preprocess/). We used the surface interpolated from the ground points that remained after filtering out vegetation as a DTM and the normalized DSM to obtain the canopy heights. We note that our study sites were flat, which likely increased the accuracy of our CHMs, relative to more topographically complex landscapes where hillslopes and micro-topography can lead to errors in plant height or, in rare cases, entirely conceal plant crowns.

Individual Plant Detection

We applied a two-step plant detection routine using the "lidR" R package (version 4.0.3; Roussel et al. 2020; Roussel & Auty 2023) to find individual plants and their size in a CHM: plant detection (i.e., individual tree detection) and plant crown delineation (i.e., segmentation). In Step 1, we used the "local maximum filter" function to detect individual plant locations based on the topography of the CHM and local height maxima using a variable window search size. To determine the search size for each pixel height, we used a linear function that approximated the allometric relationship between sagebrush height and width (width = a + b height), where a and b were linear regression parameters fit from an independent dataset. In Step

Table 1. Unoccupied aerial system (UAS) flight details for each site and time step. CHM, canopy height model.

Site	Year	UAS + Payload	Flight pattern	Side/ Front overlap (%)	Flight altitude (m)	Camera angle ()	CHM resolution (m)
Orchard	2015	senseFly eBee + Canon S110	Parallel	70/70	110	90	0.03
Orchard	2019	DJI Phantom 4 Pro + C4K 1⁰⁰ CMOS sensor	Grid	75/75	20	90 + 75	0.01
Soda	2019	DJI Matrice 600 Pro + Ricoh GRII	Grid	75/75	45	90	0.01
Soda	2021	DJI Mavic 2 Pro + Hasselblad L1D-20c	Grid	92/58	28	90 + 75	0.01

2, we delineated the crowns of individual plants using the "silva2016" region-growing algorithm and the detected points of plant locations from Step 1 (Roussel et al. 2020). We chose the input parameters for Step 1 and Step 2 using a Bayesian optimization algorithm that maximized detection and segmentation accuracy (details below). We set the minimum height threshold for the detection at 10 cm, based on the field height measurements for the plants (all plants exceeded that height except six in the Soda garden during 2019). A lower threshold would lead to a greater potential to segment spurious plants due to noise in the CHM.

The accuracy of individual plant detection and delineation is sensitive to the set of user-defined parameters in the algorithms (Ma et al. 2022; Young et al. 2022). Because individual plant detection and segmentation are computationally expensive, grid optimization becomes prohibitive as the number and range of unknown parameters increase. We implemented a Bayesian optimization algorithm from the "ParBayesianOptimization" package in R that efficiently searches for optimal parameter combinations (Frazier 2018) to minimize missed detection and over(under) segmentation of plants in the common gardens. We ran the optimization for 90 iterations, which was sufficient for the Bayesian algorithm to explore the parameter space, indicated by the error score reaching a plateau. To minimize computation time, we implemented the optimization on an area approximately 10% of the Soda garden (237 m^2) and extrapolated the optimal parameters to the entire garden for accuracy assessment and validation. The Orchard garden (675 m^2) was processed entirely, as the area was smaller compared to the Soda garden. We used field data, including total canopy cover and the number of plants in the common garden, as optimization criteria for three parameters: intercept of the allometric equation (described above), maximum cropping factor, and exclusion. The latter two are the arguments to the "silva2016" algorithm and define the crown delineation process based on the height-width allometric relationship and plant height, respectively. For each iteration of the optimization routine, the optimization used a cumulative score of the error calculated as (1) the absolute difference between the observed and modeled total canopy cover, and (2) the absolute difference between the number of observed and modeled plants in the common gardens. We ran the optimization for each dataset, to obtain a set of parameters for each year-common garden combination.

Crown-to-Crown Matching

To match crowns across time periods, we used the Jaccard Index, which calculates the percent overlap of each segmented crown (A) with each digitized crown (B) (Dalponte et al. 2019):

$$J(A,B) = \frac{|A \cap B|}{|A| + |B| - |A \cap B|} \quad \text{(Eq. 1)}$$

where $|A \cap B|$ is the area of overlap between crowns A and B. For each digitized crown, if there is one or more segmented crown that overlap across time periods, the crown with the highest Jaccard Index is assumed to be a match to the initial crown.

Survival

To estimate survival with the UAS-derived dataset, the crown-to-crown matching function was used between the two sets of segmented crowns. For remotely sensed survival, plants that were detected in both years were assumed to be alive, while plants detected in the first flight but not the second were assumed to be mortalities, and new plants only detected in the second flight were new recruits. We did not consider recruitment further in this study. Survival was calculated from field censuses that were conducted the same years as the flights. We also manually compared each set of segmented crowns and the hand-digitized crowns to assess whether they represented living sagebrush plants, dead sagebrush plants, split sagebrush crowns, merged sagebrush crowns, non-sagebrush shrubs, or bunchgrasses. Split crowns occurred when a single crown was represented by more than one segmented crown (i.e., over-segmentation). Merged crowns occurred when multiple crowns were represented as a single segmented crown (i.e., under-segmentation). These errors are captured in comparing the number of field-validated shrubs with drone-detected shrubs.

Growth

For plants that survived between the two flights, and that were segmented in both years, we compared change in crown area. Growth was assessed by subtracting the digitized crown area of the first flight from the digitized crown area of the second flight. We elected to use the digitized crown area as the reference size metric, rather than field measurements, as using hand-measured length and width to calculate area is a rougher approximation of plant canopy area than the whole-plant measurements possible with aerial imagery (Olsoy et al. 2015; Howell et al. 2020). We then compared that estimate of growth with the differenced area that was segmented during the two flights. We also report the change in maximum height between each matched pair of segmented crowns. We evaluated error for growth, a continuous variable, using Mean Absolute Error (MAE) and R^2 metrics.

Results

Plant Detection and Segmentation

The Bayesian optimization process tested a wide range of parameter space for the intercept of the allometric function and for the two segmentation parameters, with the final optimized segmentation selected by minimizing the difference between segmented and observed plant count and total canopy area. During the plant detection step, the optimal value for the intercept in the allometric equation (i.e., search window parameter) was 0.58 and 1.06 m for 2015 and 2019, respectively. In the Soda garden, the intercept values had a smaller difference between censuses, with estimated optima of 0.71 and 0.73 m for 2019 and 2021, respectively. From the full tested parameter space, the range of explored plant counts with the Bayesian optimization was 60–9827 plants (320 observed, 309 segmented) in the Orchard garden in 2015; 53–1561 plants (219 observed, 211 segmented) in the Orchard garden in 2019; 85–145 plants (114 observed, 112 segmented) in the Soda garden in 2019; and 76–257 plants (113 observed, 111 segmented) in the Soda garden in 2021. The parameter space for cover estimates during optimization similarly encompassed the field measurements, which for Orchard 2015 was 0.29–477.42 (210.9 m^2 observed area [i.e., the sum of all hand-digitized crown areas], 208.9 m^2 segmented) for Orchard 2015, 0.29–453.73 (185.36 m^2 observed area, 180.0 m^2 segmented) for Orchard 2019, 0.17–41.37 m^2 total canopy area (27.39 m^2 observed area, 26.8 m^2 segmented) for Soda 2019, and 0.05–54.92 (35.37 m^2 observed area, 35.5 m^2 segmented) for Soda 2021. The Pearson correlations between the number of detected plants and segmented canopy area across the four datasets was weak (r^2 = 0.13 to 0.20), revealing the importance of incorporating both cover- and count-based metrics when optimizing canopy segmentation from high-resolution imagery. At the Orchard garden, segmentation accuracy was 78.0% in 2015 (F-score = 0.785) and 73.3% in 2019 (F-score = 0.731; Table 2). At the Soda garden, segmentation accuracy was 95.3% in 2019 (F-score = 0.960) and 89.7% in 2021 (F-score = 0.898; Table 2).

The primary source of segmentation error at each site was different. At Orchard garden, the older, more established stand, error was due to merged plant crowns. At Soda garden, the newly established stand, plants were still evenly spaced with minimal overlap between distinct crowns, but also included small plants with heights below the minimum height threshold for detection. Out of 309 segmented shrubs, Orchard 2015 had 40 segmented crowns with multiple living shrubs within them (i.e., merged crowns), while 42 segmented crowns were of dead shrubs and 16 were split crowns (Table 3). Similarly, out of 211 segmented shrubs, Orchard 2019 had 36 crowns with merged crowns, but slightly more dead shrubs (48) with 39 of those being shrubs that died between the 2015 and 2019 flights. An additional nine segmented crowns were split crowns (Table 3). For the younger Soda garden, fewer sagebrush plants had died, so most of the error was due to non-sagebrush species that invaded the common garden (Fig. 3). Soda 2019 had 37 segmented crowns that were bunchgrasses or other non-sagebrush shrubs, with only two dead shrubs and eight merged crowns (Table 3). Soda 2021 had 118 bunchgrasses or non-sagebrush shrubs, and no split or merged crowns (Table 3).

Survival

In the Orchard garden, remotely sensed survival was 61%, with 188 individual shrubs detected in 2015 that survived to 2019, and 121 individuals shrubs in 2015 that were not detected in 2019 (Table 4). Survival from the field censuses was 70%, with 313 shrubs in 2015 and 219 shrubs in 2019 (94 mortalities). Remotely sensed survival was slightly lower than field-measured survival, but abundance was more severely underestimated with only 144 of the shrubs detected in both years that were alive in 2019 (i.e., true positive detections), and 39 detections representing dead shrubs (i.e., false positive detections; Fig. 3 and Table 3). Thirty-four of the dead shrubs had recently died (i.e., between the two UAS flights) but were already 5–8 years old and therefore well-established plants. Most of the undetected living shrubs were contained within merged crowns, with 42 crowns containing two or more living shrubs in 2019 (Table 3). In the Soda garden, remotely sensed survival was 90%, with 1082 matched crowns between years and 118 shrubs in 2019 that were not detected in 2021 (Table 4). Survival from the field censuses in the Soda garden was 99% with 1217 in 2019 and 1209 shrubs in 2021 (eight mortalities). While there were fewer errors in the Soda garden than the Orchard garden, for 2019 there were 37 segmented crowns that represented bunchgrasses or other non-target shrub species. In 2021, that increased to 118 segmented crowns that were not sagebrush (10% error; Table 3).

Growth

The shrubs in the Orchard garden grew, based on hand-digitized crowns, by an average of 0.14 m^2 (range: 0.99 to 2.10 m^2). Estimates obtained by differencing segmented crowns overestimated growth by 57% with an average 0.22 m^2 growth

Table 2. Segmentation accuracy results compared to digitized crowns for each site and time step. The plants that were digitized but not segmented are given in the third column (producer's accuracy), while the plants that were segmented but not digitized are given in the fourth column (user's accuracy), and an F-Score representing overall predictive performance.

Flight	Plants detected	Not segmented (producer's accuracy)	Not digitized (user's accuracy)	F-Score
Orchard 2015	244	69 (78.0%)	65 (79.0%)	0.785
Orchard 2019	154	56 (73.3%)	57 (73.0%)	0.731
Soda 2019	1160	57 (95.3%)	40 (96.7%)	0.960
Soda 2021	1084	125 (89.7%)	120 (90.0%)	0.898

Table 3. Survival and crown-to-crown matching accuracy confirmed with common garden census and visual inspection of high-resolution unoccupied aerial systems (UAS) imagery. Numbers refer to counts of segmented plants and percentages in parentheses represent the percent of total plants segmented in that category. The recent die-off category is for the Orchard garden because a large number of shrubs died between the 2015 and 2019 flights. Bunchgrass/Other Shrub only occurred at the Soda garden where extra crowns that were not a living shrub were often crested wheatgrass or other non-target shrub species that colonized spots where big sagebrush plants had previously died. Merged crowns occurred more frequently at the Orchard garden, where large shrub canopies combined and were more likely to be segmented as a single crown. The "matched" columns refer to crowns that were successfully paired between years with crown-to-crown matching.

	Orchard 2015	Orchard 2019	Orchard Matched	Soda 2019	Soda 2021	Soda Matched
Alive	246 (80%)	151 (72%)	144 (77%)	1161 (97%)	1085 (90%)	1053 (97%)
Dead	42 (14%)	9 (4%)	5 (3%)	2 (0%)	1 (0%)	1 (0%)
Recent Die-off	-	39 (18%)	34 (18%)	-0	-0	-0
Split Crown	16 (5%)	9 (4%)	3 (2%)	37 (3%)	118 (10%)	28 (3%)
Bunchgrass/Other Shrub	-	-	-	-1200	-1204	-1082
Border Shrub	5 (2%)	3 (1%)	2 (1%)	8	0	0
Total Crowns	309	211	188			
Merged Crowns	40	36	42			

(range: 1.90 to 2.10 m^2; Fig. 4). Individual-level growth estimates between digitized and segmentation methods were moderately correlated (MAE = 0.41 m^2, R^2 = 0.25). Shrubs that grew together and merged crowns, which were in some cases segmented as a single, much larger plant, led to high overestimation errors in growth (Fig. 3A) and is linked to the underestimation of survival. Removing segmented crowns with merged crowns decreased the MAE to 0.35 m^2 and slightly

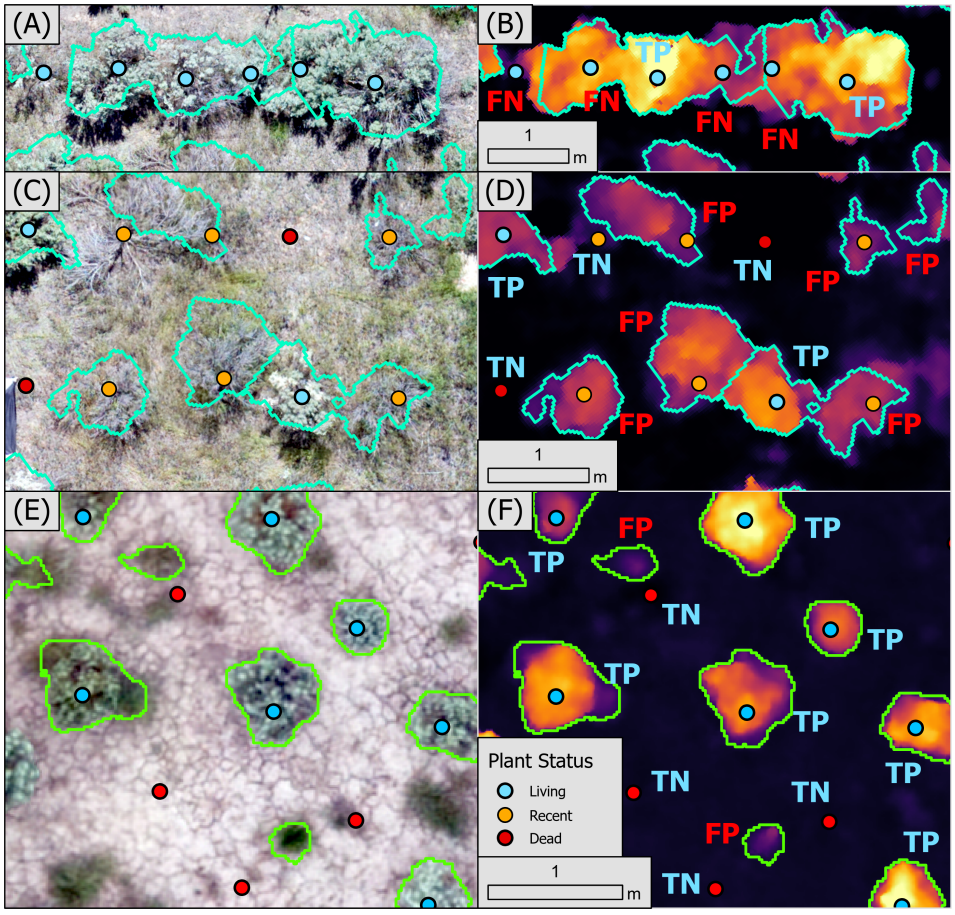

Figure 3. Examples of types of errors in segmentation and survival. UAS color (RGB) imagery (left) and CHM (right). Segmentation and survival analysis errors include merged crowns (A, B), split crowns (C, D), dead shrubs that were segmented (C, D), and bunchgrasses on non-sagebrush shrubs that were segmented (E, F). FN, false negative; FP, false positive; TN, true negative; TP, true positive. Colored points represent locations of planted sagebrush, with blue points indicating living plants, orange points for plants that died between the census surveys (recent), and red points indicating plants that were dead before the first survey.

Table 4. Remotely sensed survival estimates at each garden from direct crown-to-crown matching of segmented plants between time steps. Plants detected in both time steps are assumed to have survived, while missing plants from the first time step are assumed to have died, and new plants from the second time step are assumed to be new recruits. Validation of each year and the crown-to-crown matched subset is given in Table 3, which assesses individual-level survival accuracy.

Orchard Garden	Segmented 2015	Recruit estimate	Count 2019
Segmented 2019	188	23	211
Dead estimate	121		
Survival estimate	188/309 = 60.8%		
Soda Garden	**Segmented 2019**	**Recruit estimate**	**Count 2021**
Segmented 2021	1082	122	1204
Dead estimate	118		
Survival estimate	1082/1200 = 90.2%		

improved agreement with hand-digitized growth estimates (R^2 = 0.31). Maximum shrub height in the Orchard garden increased by an estimated 0.10 m between the two sampling dates (range: 0.46 to 0.75 m). Growth in maximum height at the Soda garden was minimal, with digitized crowns showing an average increase of 0.04 m^2 crown area (range: 0.29 to 0.39 m^2; Fig. 4). Estimated growth from the segmented crowns was 0.05 m^2 (range: 0.39 to 0.45 m^2) with MAE of 0.09 m^2 (R^2 = 0.10). Maximum height in the Soda garden decreased by 0.03 m (range: 0.40 to 0.25 m).

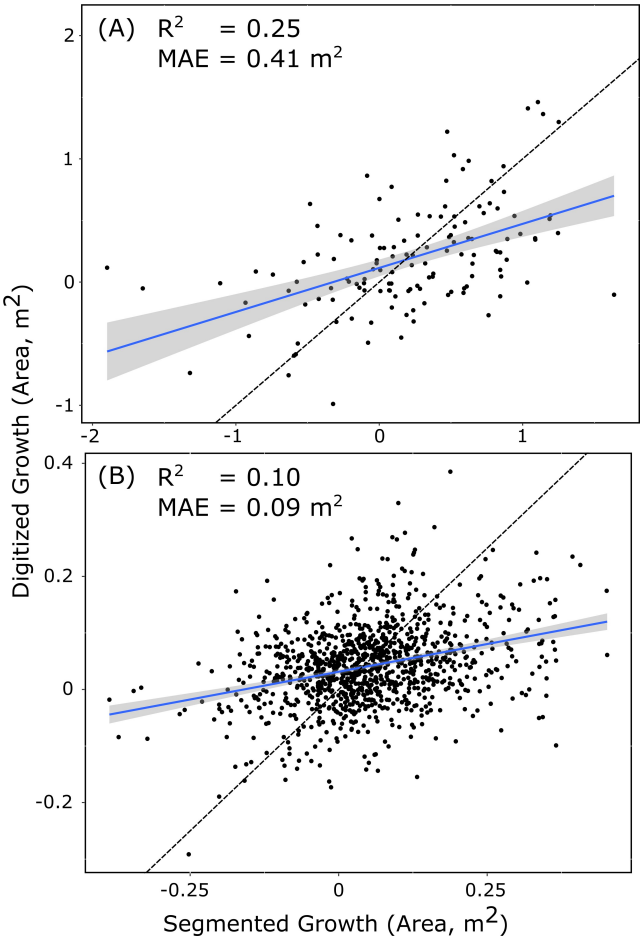

Figure 4. Area growth in segmented plants versus digitized for the Orchard (A) and Soda (B) common gardens in Idaho, USA. MAE, mean absolute error; black dashed line represents a 1:1 relationship, while the blue line represents a best-fit line to the data.

Discussion

Our work demonstrates the feasibility and errors of measuring plant demographic rates with high-resolution remotely sensed data, starting with a simplified system of shrub gardens on flat landscapes where the soils had been tilled, and background vegetation was still recovering from garden establishment. Results suggest that remote sensing that strategically reduces segmentation and classification errors can meet the demand for large-scale monitoring with relevance for restoration, from evaluating outplanting success to quantifying potential natural regeneration. Estimates of canopy structure were essential to our approach, with CHMs derived from structure from motion. The increasing availability of remotely sensed data capable of mapping 3-dimensional structure, from low-cost UAS to aerial and satellite-based LiDAR (Anderson & Gaston 2013; Olsoy et al. 2018; Ilangakoon et al. 2021), will enable similar estimates across many systems.

We found tradeoffs in optimizing segmentation for estimating the number of individual plants versus total crown area. Given the importance of accurate estimates of both plant abundance and size for demographic rates (Shriver et al. 2019), careful optimization of segmentation parameters is necessary to achieve more accurate results. The next, and most important, step for estimating growth and survival is to match segmented crowns from the same individual across time steps. We found that errors in crown-to-crown matching depended largely on the age structure of the stand. In the older stand at Orchard garden, we found that overall survival estimates were similar, but abundance estimates of matched plants were lower, largely due to crowns merging together into single segmented crowns, and potentially impacted by coarser pixel resolution (3 cm) in the 2015 flight. For the younger stand at Soda garden, survival and abundance

estimates were very close, and the errors were driven by segmentation of non-target plants. Monitoring the extent and timing of merged plants through multiple time steps and classification of species is needed to assess how mixed-age stands along the edges of disturbance (e.g., wildfire boundaries) impact segmentation accuracy and demographic rate estimates.

For a single time step, we found that segmentation performed well, including fairly accurate estimates of cover and plant abundance. Counts of individual plants and cover estimates are essential for many ecological applications, from predicting future population growth to measuring potential forage for threatened herbivores (Olsoy et al. 2020; Barber et al. 2022). Estimating plant population dynamics with remote sensing, including forecasting cover trajectories and population growth rate, will require integrating measurements across years. We found that crown-to-crown matching across time steps was a considerably more difficult challenge than single-year estimation of sagebrush crown segments. Misclassifications or merged crowns upstream in the workflow were compounded by crown-to-crown matching. At Orchard, 1 year had more individual crowns merged together, and our crown-to-crown matching algorithm only matches the crown with the most overlap leading to an underestimation in abundance, possible overestimation of mortalities, and increased errors in growth estimates. While our study was part of a common garden experiment, natural systems closer to carrying capacity that contain older plants will likely also have this problem, as canopies expand and eventually overlap. Other studies have adjusted for over- and under-segmentation with spectral approaches (Zhang et al. 2012). Stands recovering from fire or other disturbances are likely to begin more sparsely distributed with small seedlings that are harder to detect with remote sensing than larger plants. Segmentation parameters can be optimized to detect smaller plants, but in our case that led to false positives with bunchgrasses and other small, non-target plants being segmented. Spectral information could be used to classify segmented crowns to species and reduce misidentification errors, particularly multispectral and hyperspectral sensors that are becoming more common on UAS platforms (van Blerk et al. 2022; Slade et al. 2023).

Despite the challenges of crown-to-crown matching, we were able to achieve fairly accurate estimates of stand-level survival with remotely sensed estimates within 10% of observed survival. Mortality of outplants can lead to failure of active restoration projects (Davidson et al. 2019). For large-scale restoration projects, such as mass tree planting efforts, insufficient monitoring of outplant survival is common and poses a major impediment to improving the success of subsequent plantings through adaptive management (Brancalion & Holl 2020). Remotely sensed data, including UAS imagery, could provide a low-cost and scalable solution to the challenge of monitoring outplant survival across large areas. We anticipate that estimating the survival of naturally regenerating plants with UAS imagery will be more difficult than our case study, which involved regularly spaced outplants in a common garden. Continued improvement of segmentation algorithms will potentially improve crown-to-crown matching. However, in other cases, models that combine field measurements of mortality for a subsample of plants with large-scale remotely sensed estimates may be necessary for best performance (Barber 2021).

In contrast to survival, we found growth more challenging to estimate with UAS imagery. Growth rates in older gardens may be overestimated due to merged canopies, and growth rates in younger gardens may require longer time steps. Despite these challenges, we were able to detect a significant relationship between remotely estimated growth and hand-digitized growth of tagged shrubs. This overall positive relationship points to the potential capacity to improve estimates of growth for outplants with improved segmentation algorithms. Alternately, if accurate estimates of growth are needed from remotely sensed imagery, hand-digitization and subsequent pairing of digitized crowns is a feasible, albeit time-consuming, solution (Stears et al. 2022). Estimating growth may also be easier for plants with simpler canopy structure than sagebrush shrubs, where irregular, asymmetric, and disjoint canopies are the norm, particularly for older plants.

Across our entire workflow, we anticipate that multispectral or hyperspectral data could be leveraged to reduce errors (Qin et al. 2022). Additional spectral resolution improves the ability to classify plant crowns to species, potentially removing errors in crown-to-crown matching due to confusion between focal species and others. Species classification will be particularly important in natural settings, where plant diversity is higher than our common garden case study. Another way that multispectral sensors could aid the detection of growth and survival is by measuring spectral changes in plant crowns that can predict demographic changes (Caughlin et al. 2016). For example, plants that are likely to die may have less spectral reflectance in photosynthetically active bands. Other potential examples of within-crown spectral variability with relevance for demography could include reproductive seed heads or leaf stress. Moreover, alignment of UAS imagery with the timing of leaf emergence and senescence may also help classify species. Multispectral sensors are becoming cheaper and more available on UAS, and offer the opportunity to assist with species classification and plant physiology and disease (Tu et al. 2019).

Models for imperfect detection present another possible avenue to improve remotely sensed estimates of plant demography. Hierarchical models that partition noisy data into measurement error and process variability are common in wildlife studies and have enabled inference on animal demography from camera trap data, which poses similar detectability challenges to UAS imagery. Adapting these hierarchical models for plant detection from UAS imagery is feasible, including simultaneously estimating the probability of false negatives (failure to detect a focal plant, when one is present) and false positives (incorrect detection due to species misclassification, split crowns, or error in the CHM) (Zaiats et al. 2023), and explicitly modeling detection probabilities is likely to improve demographic estimates, particularly for smaller plants.

The technical expertise required to acquire and process remotely sensed data raises the question of when remote sensing estimates will sufficiently decrease monitoring cost to become feasible, relative to field data. We anticipate that the answer to this question will depend in part on the scale of monitoring

needed. For large-scale restoration treatments, such as many post-fire efforts in the Great Basin (Simler-Williamson & Germino 2022), full censuses are logistically infeasible. Subsampling large areas with field plots is one solution, but the lack of spatially extensive measurements presents an impediment to efforts to spatially-target subsequent restoration treatments to areas that are underperforming. An additional benefit of remotely sensed imagery is the capacity for flexible deployment and image acquisition, in response to disturbance and phenological events (Bogdan et al. 2021; Gonzales et al. 2022). For arid or semi-arid systems where plants are only visible for brief phenological windows, field surveys may underrepresent counts of crucial functional groups (Endress et al. 2022). An alternative approach to our workflow that could potentially reduce the technical costs of segmentation and crown-to-crown matching would be to produce data products that represent aggregate cover and count metrics, rather than survival and growth of individuals. In some cases, time series of plant cover can provide more accurate forecasts of future population dynamics (Tredennick et al. 2017). We found that stand-level estimates of plant cover or counts were more accurate than products that required crown-to-crown matching. Additionally, cover estimates are now possible with satellite imagery leading to opportunities for long-term and historic estimates of population dynamics that are not possible with UAS imagery alone (Zaiats et al. 2023). However, in other cases, estimates of individual demography may be required. For example, experimental outplants designed to test the performance of different genotypes or functional traits, such as the common garden data analyzed in this paper, require analysis at an individual level (Rincent et al. 2018).

Ultimately, as the cost and accessibility of UAS technology continue to decline, we anticipate that high-resolution UAS will increasingly bridge the gap in scale between field-based measurements of individual plants and satellite-based fractional cover estimates. Our semi-automated segmentation provides an example of low-cost drone mapping that can enable the detection and mapping of thousands to hundreds of thousands of individual plants in a single flight. Land managers could use UAS to capture multiple time steps (e.g., annual or after multiple years) to monitor growth and survival of targeted species and assess restoration outcomes at broad scales. Initial segmentation and classification algorithms require an upfront cost, but as workflows become more automated, the cost decreases and UAS data collection can often be cheaper and easier than time-intensive fieldwork.

Acknowledgments

NSF Idaho track 1 EPSCoR Program and National Science Foundation OIA-1757324 and OIA-1826801. T. Trevor Caughlin was funded by NSF BIO-2207158. Thanks to D. Pfeifer, R. Schumaker, and the Idaho EPSCoR staff for administrative support on this project. Thanks to S. Galla for artwork included in the workflow diagram. Funding for common garden installation and cytotyping: Joint Fire Science Program, Great Basin Native Plant Project and USDA Forest Service, Rocky Mountain Research Station. Any use of trade, firm, or product names is for descriptive purposes only and does not imply endorsement by the U.S. Government.

Data Availability Statement

The data that support the findings of this study are openly available from the University of Idaho at https://doi.org/10.7923/xj7r-1d86.

LITERATURE CITED

Albrecht MA, McCue KA (2010) Changes in demographic processes over long time scales reveal the challenge of restoring an endangered plant. Restoration Ecology 18:235–243. https://doi.org/10.1111/j.1526-100X.2009.00584.x

Anderson K, Gaston KJ (2013) Lightweight unmanned aerial vehicles will revolutionize spatial ecology. Frontiers in Ecology and the Environment 11:138–146. https://doi.org/10.1890/120150

Barber C (2021) Upscaling tree demography to heterogenous landscapes using models and remote sensing. Boise State University Theses and Dissertations

Barber C, Graves SJ, Hall JS, Zuidema PA, Brandt J, Bohlman SA, Asner GP, Bailon M, Caughlin TT (2022) Species-level tree crown maps improve predictions of tree recruit abundance in a tropical landscape. Ecological Applications 32:e2585. https://doi.org/10.1002/eap.2585

Beese L, Dalponte M, Asner GP, Coomes DA, Jucker T (2022) Using repeat airborne LiDAR to map the growth of individual oil palms in Malaysian Borneo during the 2015–16 El Niño. International Journal of Applied Earth Observation and Geoinformation 115:103117. https://doi.org/10.1016/j.jag.2022.103117

Bogdan A, Levin SC, Salguero-Gomez R, Knight TM (2021) Demographic analysis of an Israeli Carpobrotus population. PLoS One 16:e0250879. https://doi.org/10.1371/journal.pone.0250879

Brancalion PHS, Holl KD (2020) Guidance for successful tree planting initiatives. Journal of Applied Ecology 57:2349–2361. https://doi.org/10.1111/1365-2664.13725

Brandt M, Tucker CJ, Kariryaa A, Rasmussen K, Abel C, Small J, et al. (2020) An unexpectedly large count of trees in the West African Sahara and Sahel. Nature 587:78–82. https://doi.org/10.1038/s41586-020-2824-5

Caughlin TT, de la Peña-Domene M, Martínez-Garza C (2019) Demographic costs and benefits of natural regeneration during tropical forest restoration. Ecology Letters 22:34–44. https://doi.org/10.1111/ele.13165

Caughlin TT, Elliott S, Lichstein JW (2016) When does seed limitation matter for scaling up reforestation from patches to landscapes? Ecological Applications 26:2439–2450. https://doi.org/10.1002/eap.1410

Dalponte M, Frizzera L, Gianelle D (2019) Individual tree crown delineation and tree species classification with hyperspectral and LiDAR data. PeerJ 6:e6227. https://doi.org/10.7717/peerj.6227

Davidson BE, Germino MJ (2020) Spatial grain of adaptation is much finer than ecoregional-scale common gardens reveal. Ecology & Evolution 10:9920–9931. https://doi.org/10.1002/ece3.6651

Davidson BE, Germino MJ, Richardson B, Barnard DM (2019) Landscape and organismal factors affecting sagebrush-seedling transplant survival after megafire restoration. Restoration Ecology 27:1008–1020. https://doi.org/10.1111/rec.12940

Endress BA, Averett JP, Steinmetz S, Quaempts EJ (2022) Forgotten forbs: standard vegetation surveys underrepresent ecologically and culturally important forbs in a threatened grassland ecosystem. Conservation Science and Practice 4:e12813. https://doi.org/10.1111/csp2.12813

Frazier PI (2018) Bayesian optimization. Pages 255–278. In: Recent advances in optimization and modeling of contemporary problems. INFORMS TutORials in Operations Research INFORMS, Phoenix, AZ

Fremgen-Tarantino MR, Peña JJ, Connelly JW, Forbey JS (2020) Winter foraging ecology of Greater Sage-Grouse in a post-fire landscape. Journal of Arid Environments 178:104154. https://doi.org/10.1016/j.jaridenv.2020.104154

Frye GG, Connelly JW, Musil DD, Forbey JS (2013) Phytochemistry predicts habitat selection by an avian herbivore at multiple spatial scales. Ecology 94:308–314. https://doi.org/10.1890/12-1313.1

Germino MJ, Torma P, Fisk MR, Applestein CV (2022) Monitoring for adaptive management of burned sagebrush-steppe rangelands: addressing variability and uncertainty on the 2015 Soda Megafire. Rangelands 44:99–110. https://doi.org/10.1016/j.rala.2021.12.002

Gillan JK, Karl JW, van Leeuwen WJD (2020) Integrating drone imagery with existing rangeland monitoring programs. Environmental Monitoring and Assessment 192:269. https://doi.org/10.1007/s10661-020-8216-3

Godefroid S, Piazza C, Rossi G, Buord S, Stevens A-D, Aguraiuja R, et al. (2011) How successful are plant species reintroductions? Biological Conservation 144:672–682. https://doi.org/10.1016/j.biocon.2010.10.003

Gonzales D, Hempel de Ibarra N, Anderson K (2022) Remote sensing of floral resources for pollinators – new horizons from satellites to drones. Frontiers in Ecology and Evolution 10:869751. https://doi.org/10.3389/fevo.2022.869751

Holl KD (1999) Factors limiting tropical rain forest regeneration in abandoned pasture: seed rain, seed germination, microclimate, and soil. Biotropica 31:229–242. https://doi.org/10.1111/j.1744-7429.1999.tb00135.x

Holl KD, Brancalion PHS (2020) Tree planting is not a simple solution. Science 368:580–581. https://doi.org/10.1126/science.aba8232

Hoover DL, Bestelmeyer B, Grimm NB, Huxman TE, Reed SC, Sala O, Seastedt TR, Wilmer H, Ferrenberg S (2020) Traversing the wasteland: a framework for assessing ecological threats to drylands. Bioscience 70:35–47. https://doi.org/10.1093/biosci/biz126

Howell RG, Jensen RR, Petersen SL, Larsen RT (2020) Measuring height characteristics of sagebrush (Artemisia sp.) using imagery derived from small unmanned aerial systems (sUAS). Drones 4:6. https://doi.org/10.3390/drones4010006

Ilangakoon N, Glenn NF, Schneider FD, Dashti H, Hancock S, Spaete L, Goulden T (2021) Airborne and spaceborne lidar reveal trends and patterns of functional diversity in a semi-arid ecosystem. Frontiers in Remote Sensing 2:743320. https://doi.org/10.3389/frsen.2021.743320

James JJ, Svejcar TJ, Rinella MJ (2011) Demographic processes limiting seedling recruitment in arid grassland restoration. Journal of Applied Ecology 48:961–969. https://doi.org/10.1111/j.1365-2664.2011.02009.x

Kalacska M, Sanchez-Azofeifa GA, Rivard B, Caelli T, White HP, Calvo-Alvarado JC (2007) Ecological fingerprinting of ecosystem succession: estimating secondary tropical dry forest structure and diversity using imaging spectroscopy. Remote Sensing of Environment 108:82–96. https://doi.org/10.1016/j.rse.2006.11.007

Ma K, Chen Z, Fu L, Tian W, Jiang F, Yi J, Du Z, Sun H (2022) Performance and sensitivity of individual tree segmentation methods for UAV-LiDAR in multiple forest types. Remote Sensing 14:298. https://doi.org/10.3390/rs14020298

Marconi S, Weinstein BG, Zou S, Bohlman SA, Zare A, Singh A, Stewart D, Harmon I, Steinkraus A, White EP (2022) Continental-scale hyperspectral tree species classification in the United States National Ecological Observatory Network. Remote Sensing of Environment 282:113264. https://doi.org/10.1016/j.rse.2022.113264

Merow C, Dahlgren JP, Metcalf JE, Childs DZ, Evans MEK, Jongejans E, Record S, Rees M, Salguero-Gomez R, McMahon SM (2014) Advancing population ecology with integral projection models: a practical guide. Methods in Ecology and Evolution 5:99–110. https://doi.org/10.1111/2041-210X.12146

Olsoy PJ, Forbey JS, Rachlow JL, Nobler JD, Glenn NF, Shipley LA (2015) Fearscapes: mapping functional properties of cover for prey with terrestrial LiDAR. Bioscience 65:74–80. https://doi.org/10.1093/biosci/biu189

Olsoy PJ, Forbey JS, Shipley LA, Rachlow JL, Robb BC, Nobler JD, Thornton DH (2020) Mapping foodscapes and sagebrush morphotypes with unmanned aerial systems for multiple herbivores. Landscape Ecology 35:921–936. https://doi.org/10.1007/s10980-020-00990-1

Olsoy PJ, Shipley LA, Rachlow JL, Forbey JS, Glenn NF, Burgess MA, Thornton DH (2018) Unmanned aerial systems measure structural habitat features for wildlife across multiple scales. Methods in Ecology and Evolution 9:594–604. https://doi.org/10.1111/2041-210X.12919

Osinska-Skotak K, Radecka A, Piorkowski H, Michalska-Hejduk D, Kopec D, Tokarska-Guzik B, Ostrowski W, Kania A, Niedzieko J (2019) Mapping succession in non-forest habitats by means of remote sensing: is the data acquisition time critical for species discrimination? Remote Sensing 11:2629. https://doi.org/10.3390/rs11222629

Peter BG, Messina JP (2019) Errors in time-series remote sensing and an open access application for detecting and visualizing spatial data outliers using Google earth engine. IEEE Journal of Selected Topics in Applied Earth Observations and Remote Sensing 12:1165–1174. https://doi.org/10.1109/JSTARS.2019.2901404

Pilliod DS, Welty JL, Toevs GR (2017) Seventy-five years of vegetation treatments on public rangelands in the Great Basin of North America. Rangelands 39:1–9. https://doi.org/10.1016/j.rala.2016.12.001

Qin H, Zhou W, Yao Y, Wang W (2022) Individual tree segmentation and tree species classification in subtropical broadleaf forests using UAV-based LiDAR, hyperspectral, and ultrahigh-resolution RGB data. Remote Sensing of Environment 280:113143. https://doi.org/10.1016/j.rse.2022.113143

Requena-Mullor JM, Brandt J, Williamson MA, Caughlin TT (2023) Human population growth and accessibility from cities shape rangeland condition in the American West. Landscape and Urban Planning 232:104673. https://doi.org/10.1016/j.landurbplan.2022.104673

Richardson BA, Chaney L (2018) Climate-based seed transfer of a widespread shrub: population shifts, restoration strategies, and the trailing edge. Ecological Applications 28:2165–2174. https://doi.org/10.1002/eap.1804

Rincent R, Charpentier JP, Faivre-Rampant P, Paux E, Le Gouis J, Bastien C, Segura V (2018) Phenomic selection is a low-cost and high-throughput method based on indirect predictions: proof of concept on wheat and poplar. G3: Genes, Genomes, Genetics 8:3961–3972. https://doi.org/10.1534/g3.118.200760

Rominger K, Meyer SE (2019) Application of UAV-based methodology for census of an endangered plant species in a fragile habitat. Remote Sensing 11:719. https://doi.org/10.3390/rs11060719

Roser A, Enterkine J, Requena-Mullor JM, Glenn NF, Boehm A, de Graaff M-A, Clark PE, Pierson F, Caughlin TT (2022) Drone imagery protocols to map vegetation are transferable between dryland sites across an elevational gradient. Ecosphere 13:e4330. https://doi.org/10.1002/ecs2.4330

Roussel J-R, Auty D (2023) Airborne LiDAR data manipulation and visualization for forestry applications. R package version 4.0.3. https://cran.r-project.org/package=lidR

Roussel J-R, Auty D, Coops NC, Tompalski P, Goodbody TRH, Meador AS, Bourdon J-F, de Boissieu F, Achim A (2020) lidR: an R package for analysis of Airborne Laser Scanning (ALS) data. Remote Sensing of Environment 251:112061. https://doi.org/10.1016/j.rse.2020.112061

Sankey TT, Sankey JB, Horne R, Bedford A (2016) Remote sensing of tamarisk biomass, insect herbivory, and defoliation: novel methods in the Grand Canyon Region, Arizona. Photogrammetric Engineering & Remote Sensing 82:645–652. https://doi.org/10.14358/PERS.82.8.645

Shriver RK, Andrews CM, Arkle RS, Barnard DM, Duniway MC, Germino MJ, Pilliod DS, Pyke DA, Welty JL, Bradford JB (2019) Transient population dynamics impede restoration and may promote ecosystem transformation after disturbance. Ecology Letters 22:1357–1366. https://doi.org/10.1111/ele.13291

Simler-Williamson AB, Germino MJ (2022) Statistical considerations of nonrandom treatment applications reveal region-wide benefits of widespread post-fire restoration action. Nature Communications 13:3472. https://doi.org/10.1038/s41467-022-31102-z

Slade G, Fawcett D, Cunliffe AM, Brazier RE, Nyaupane K, Mauritz M, Vargas S, Anderson K (2023) Optical reflectance across spatial scales–an intercomparison of transect-based hyperspectral, drone, and satellite reflectance data for dry season rangeland. Drone Systems and Applications 11:1–20. https://doi.org/10.1139/dsa-2023-0003

Stears AE, Adler PB, Albeke SE, Atkins DH, Studyvin J, Laughlin DC (2022) plantTracker: an R package to translate maps of plant occurrence into demographic data. Methods in Ecology and Evolution 13:2129–2137. https://doi.org/10.1111/2041-210X.13950

Tompalski P, Coops NC, White JC, Goodbody TRH, Hennigar CR, Wulder MA, Socha J, Woods ME (2021) Estimating changes in forest attributes and enhancing growth projections: a review of existing approaches and future directions using airborne 3D point cloud data. Current Forestry Reports 7:1–24. https://doi.org/10.1007/s40725-021-00135-w

Tredennick AT, Hooten MB, Adler PB (2017) Do we need demographic data to forecast plant population dynamics? Methods in Ecology and Evolution 8: 541–551. https://doi.org/10.1111/2041-210X.12686

Tu Y-H, Johansen K, Phinn S, Robson A (2019) Measuring canopy structure and condition using multi-spectral UAS imagery in a horticultural environment. Remote Sensing 11:269. https://doi.org/10.3390/rs11030269

Ulappa AC, Kelsey RG, Frye GG, Rachlow JL, Shipley LA, Bond L, Pu X, Forbey JS (2014) Plant protein and secondary metabolites influence diet selection in a mammalian specialist herbivore. Journal of Mammalogy 95:834–842. https://doi.org/10.1644/14-MAMM-A-025

van Blerk JJ, West AG, Smit J, Altwegg R, Hoffman MT (2022) UAVs improve detection of seasonal growth responses during post-fire shrubland recovery. Landscape Ecology 37:3179–3199. https://doi.org/10.1007/s10980-022-01535-4

Williams J, Jackson TD, Schönlieb C-B, Swinfield T, Irawan B, Achmad E, Zudhi M, Habibi H, Gemita E, Coomes DA (2022) Monitoring early-successional trees for tropical forest restoration using low-cost UAV-based species classification. Frontiers in Forests and Global Change 5:87644. https://doi.org/10.3389/ffgc.2022.876448

Williams J, Schönlieb C-B, Swinfield T, Lee J, Cai X, Qie L, Coomes DA (2020) 3D segmentation of trees through a flexible multiclass graph cut algorithm. IEEE Transactions on Geoscience and Remote Sensing 58:754–776. https://doi.org/10.1109/TGRS.2019.2940146

Young DJN, Koontz MJ, Weeks J (2022) Optimizing aerial imagery collection and processing parameters for drone-based individual tree mapping in structurally complex conifer forests. Methods in Ecology and Evolution 13:1447–1463. https://doi.org/10.1111/2041-210X.13860

Zaiats A, Cattau ME, Pilliod DS, Liu R, Requena-Mullor JM, Caughlin TT (2023) Forecasting natural regeneration of sagebrush after wildfires using population models and spatial matching. Landscape Ecology 38:1291–1306. https://doi.org/10.1007/s10980-023-01621-1

Zhang W, Quackenbush LJ, Im J, Zhang L (2012) Indicators for separating undesirable and well-delineated tree crowns in high spatial resolution images. International Journal of Remote Sensing 33:5451–5472. https://doi.org/10.1080/01431161.2012.663109

Zhao K, Suarez JC, Garcia M, Hu T, Wang C, Londo A (2018) Utility of multitemporal lidar for forest and carbon monitoring: tree growth, biomass dynamics, and carbon flux. Remote Sensing of Environment 204: 883–897. https://doi.org/10.1016/j.rse.2017.09.007

Coordinating Editor: Klaus Kellner

Received: 25 September, 2023; First decision: 13 December, 2023; Revised: 3 January, 2024; Accepted: 8 January, 2024